



# Selection of Erosive Wear Rate Parameters of Pelton Turbine Buckets using PSI and TOPSIS Techniques

Robin Thakur, Sunil Kumar, Kamal Kashyap, Ashwani Kumar, Sorabh Aggarwal

**Abstract:** Hydro turbine machineries erosion due to silt is a complex issue for the effective practice of hydropower plants. Erosion caused by silt of the Pelton turbine buckets is a compound phenomenon that depends on size of silt particles ( $S_p$ ), silt particles concentration ( $C_s$ ), velocity of jet ( $V_j$ ), and working time ( $t_w$ ). This paper deals with the influence of silt erosion for various silt loaded factors and effective parameters. The preference selection index (PSI) and technique for order of preference by similarity to ideal solution (TOPSIS) approaches has been adopted to find optimal set of parameters which offers the highest performance for the Pelton turbine. Based up on the results obtained from both PSI and TOPSIS approaches it is found that optimal performance has been provided by A-1 alternate with geometric and flow parameters as  $S_p = 90 \mu$ ,  $C_s = 2000 \text{ ppm}$ ,  $V_j = 27.309 \text{ m/s}$  and  $t_w = 3 \text{ hrs}$  respectively.

**Keywords:** Hydro energy, silt size, Pelton turbine, PSI, TOPSIS

## Nomenclature

$b$	Length of the weir crest (perpendicular to flow), (m)
$b_e$	Effective width, (m)
$C_e$	Coefficient of discharge
$C_s$	Concentration of silt particles, (ppm)
$g$	Acceleration due to gravity, $\text{m/s}^2$
$h$	Measured upstream head over the weir, (m)
$h_e$	Effective head, (m)
$H$	Net head, (m)
$k_b$	Width correction factor
$k_h$	Head correction factor
$k_v$	Velocity coefficient (= 0.98 as 2% losses are considered in the nozzle)
$P$	Pressure, (kPa)
$Q$	Discharge, ( $\text{m}^3/\text{s}$ )
$S_p$	Size of silt particles, microns ( $\mu$ )

$t_w$	Working time, (hrs)
$V$	Jet velocity in ( $\text{m/s}$ )
$V_j$	Velocity of jet, ( $\text{m/s}$ )
$\rho$	Density of water ( $\text{kg/m}^3$ )

## I. INTRODUCTION

Hydropower plants are the most progressive and established renewable energy technology and provides some level of power generation in more than 160 countries globally. Power generated from hydro has very slight environmental and social impact if we will compare it to other renewable energy resources by Singh and Singhal [1] and Robb [2]. Hydropower is the main renewable electrical energy source at universal level and contributes to sustainable progress. Hydropower is able to supply clean and reasonable energy in its most valuable form, electricity. Hydro turbine is suppose to be primary segment of a hydro control plant but regrettably, hydro turbines experience issues like sediment erosion which declines the proficiency over a time of their functioning life. Residue erosion occurrence in hydro turbine is real issue ,as it effects the smooth functioning of hydropower plants by Bansal et al. [3] and Pundir and Kumar [4].

Several experimental and analytical investigations for the deteriorated efficiency and performance of the hydro turbines due to silt erosion have been suggested and discussed by various investigators. Woodcock and White [5] studied the basics of a Pelton turbine, single-wheel development and close running clearances absence makes it more appropriate for applications. Their outcomes showed that the Pelton turbines have been employed for a long time in high-head hydroelectric power plants and high water powered production.

Chattopadhyay [6] did observation of runners from different water samples of different rivers having high silt content and observe that the wear occurred is unusual in the runners of the turbine. Their conclusions are described against microstructure, hardness and work-hardening rate based on the various wear rates of the alloys. Mann [7] examined the matter of erosion in various hydel power locations situated in Himalayan area. Mann & Arya [8] stated the abrasion and silt erosion features of HVOF coatings and plasma nitriding beside with usually used steels in hydel turbines. Their outcomes show that the HVOF tungsten carbide on steel seems, by all accounts, to be an outstanding disintegration protection shield to battle with low and high-energy molecule impingement wear.

Revised Manuscript Received on November 30, 2019.

\* Correspondence Author

**Robin Thakur\***, School of Mechanical & Civil Engineering, Shoolini University, Solan, India. Email: [robinthakur@shooliniuniversity.com](mailto:robinthakur@shooliniuniversity.com)

**Sunil Kumar**, School of Computer- Science & Electrical Engineering Shoolini University, Solan, India. -. Email: [sunilthakur@shooliniuniversity.com](mailto:sunilthakur@shooliniuniversity.com)

**Kamal Kashyap**, School of Mechanical & Civil Engineering, Shoolini University, Solan, India. Email: [kamal.maximus23@gmail.com](mailto:kamal.maximus23@gmail.com)

**Ashwani Sharma**, School of Computer- Science & Electrical Engineering Shoolini University, Solan, India. -. Email: [ashwanisharma@shooliniuniversity.com](mailto:ashwanisharma@shooliniuniversity.com)

**Sorabh Aggarwal**, School of Mechanical & Civil Engineering, Shoolini University, Solan, India. Email: [sorabh.btech11@gmail.com](mailto:sorabh.btech11@gmail.com)

© The Authors. Published by Blue Eyes Intelligence Engineering and Sciences Publication (BEIESP). This is an open access article under the CC-BY-NC-ND license <http://creativecommons.org/licenses/by-nc-nd/4.0/>

## Selection of Erosive Wear Rate Parameters of Pelton Turbine Buckets using PSI and TOPSIS Techniques

Desale, Gandhi, & Jain [9] analyzed the influence of erodent properties on slurry erosion. The investigation shows that with the reduction in the shape factor, there is a rise in wear and in the density. Bajracharya et al. [10] investigated that erosion of hydro turbine machineries is one of the complex trouble especially in monsoon season through silt in the Himalayan region. Chauhan et al. [11] observed that cavitation, material defects, fatigue and sand erosion are the major reasons for the damaging of hydro turbines in hilly terrain. Agar & Rasi [12] portrayed the development of the Pelton turbine, the test contraption and the estimation strategy. They concluded that the Pelton turbine and mechanical assembly show the standards of hydropower and are suitable for instruction in renewable power source.

Padhy & Saini [13] studied the erosive wear of hydro turbine machineries which mainly relies on various parameters, for example, size of buckets, rigidity and consideration of residue particles, jet velocity, properties of metal used as base material and the period of time a turbine works continuously. Thapa, Thapa, & Dahlhaug [14] concluded that, remarkable erosion is found on the needle rather than on the buckets which mainly occurs due to fine silt particles. [15] Numerical approach is established for a fast and actual simulation and investigation of the complex flow and energy conversion in Pelton turbines. Goyal et al. [16] did his all observations with the help of a high-speed erosion test rig developed by his own and used it for different tests based on slurry erosion, he give his observations based on speed, average particle size and slurry concentration.

Padhy & Saini [17] also reviewed various erosion models, case studies related to erosion of hydro turbine components and also investigated experimentally the erosive wear in the hydro turbine machineries. Williamson et al. [18] take 3.5 m to 1 m low head observations, the motion of a single jet Turgo turbine outside of its ordinary application area is investigated in which a regular head run accessible for remote groups. Cobb & Sharp [19] tested the working execution qualities of impulse turbines examined through the assembling of research center scale test installation. The outcomes stretch the significance of legitimate framework design and establishment and increment the learning base with respect to Turgo turbine execution that can prompt better reasonable usage in pico-hydro frameworks.

Khurana & Goel [20] analyzed experimentally erosive wear of hydro turbine segments and found that it is a critical phenomenon which mainly relies on various factors, like *size of silt particles ( $s$ )*, *silt concentration ( $c$ )*, *jet velocity ( $v$ )*, *hardness of silt particles ( $H$ )*, *properties of base materials, jet diameter ( $d$ )*, and *working hours ( $t$ )*. Platero et al. [21] discuss the novel procedure for Pelton turbine task without the use of water stream, as a methodology to give rapid power infusion on account of an unpredicted wind power diminish, or a wind generator trip. Židonis & Aggidis [22] uses commercially available CFD code fluent to accomplish an analysis of flow inside the bucket of a Pelton turbine and confirmed the results experimentally. Kumar & Bhingole, 2015 [23] have applied a simulated flow on stationary flat plate and make it functional on Kaplan turbine.

Kumar & Singal [24] discuss that the hydraulic turbine is an imperative segment in hydro power plants and it has numerous issues which degrade its condition and proficiency

and require appropriate operation and upkeep. Chávez et al. [25] examined the performance of a Pelton turbine runner comprises of 16 buckets on its periphery from a hydroelectric plant having two turbo generators with a minimal capacity of 2.33 MW each, located in Colombia. Židonis et al. [26] uses commercially available ANSYS CFX code to perform flow analysis inside stationary Pelton turbine bucket and confirmed the results experimentally. Židonis & Aggidis [27] make a numerical analysis presented by sorting the best arrangement of the radial and angular position for each bucket in which it is showed that lessening in the quantity of buckets.

Nguyen et al. [28] analyzed the particles formed by cavitation erosion and stated that many particles were quite uneven in shape. Gupta et al. [29] utilizing water and air as working fluid to examine the Pelton turbine to evaluate the productivity, blade loading, jet velocity and water appropriation over the bucket at various working segments of the turbine. Vessaz et al. [30] has optimizing the performance of a Pelton turbine runner relies on a parametric model of the bucket geometry, innovative optimization strategies and numerical simulations of massive particles. Egusquiza et al. [31] presented a process for the estimation of erosion characteristic of a hydro turbine runner under different situations. Morales B et al. [32] accomplished an experiment related to cavitation on a Pelton turbine. Kishor et al. [33] examined the impact of particle size and shape on hydraulic turbine components.

As Multiple Criteria Decision Making (MCDM) techniques are numerical methodologies for taking care of problems comprising a substantial number of options and execution assessment standards and have gotten open acknowledgment for application in different zones of science, building, administration and so on Maniya & Bhatt [34], Chauhan et al. [35], Vahdani et al. [36]. There are various MCDM techniques which are accessible in the writing to empower the inventors to assemble the superior option, in most of these techniques, the alternative rankings are influenced by the measure weight and are very strenuous to fathom and cloud to execute needful widespread mathematical complexity. It contains several strategies, specifically, grey relation analysis, preference ranking organization method for enrichment evaluations, elimination and choice translating reality, compromise ranking method, technique for order preference by similarity to ideal solutions and analytic hierarchy method which have been effectively used to take care of numerous decision-making issues Attri et al. [37], Mesran et al. [38] and Madić et al. [39].

The PSI approach is more generalized to understand as compared to all MCDM techniques as it doesn't contain any comparative importance between the standards and the overall preference value which is attained by using the statistical concept. The superiority of PSI technique is that it is useful in estimation of ideal elective where there is conflict in choosing the relative significance between the foundations and contains less numerical computations by Lockwood [40] and Maniya & Bhatt [41]. The methodology for order preference by similarity to an ideal solution (TOPSIS) technique is useful for decision makers to structure the problems to be sort out, conduct analyses, comparisons and ranking of the alternatives [42].



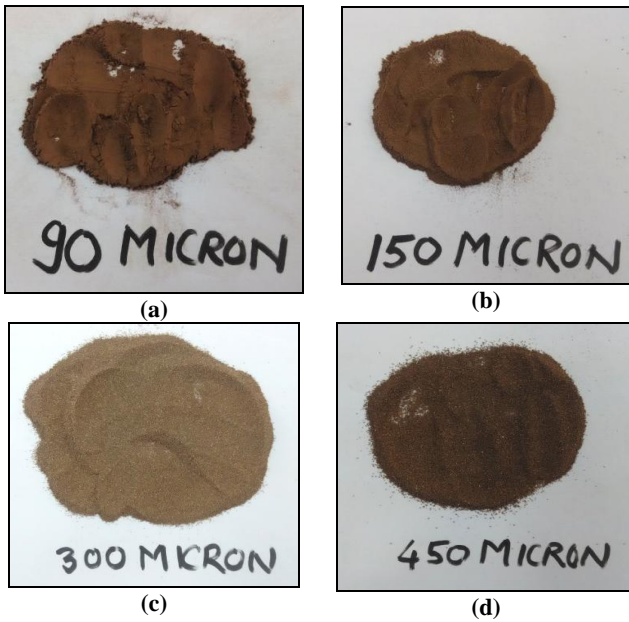


Figure 4. Silt samples of various sizes of Chamera dam

Table 1 Range of experimental parameters

Sr. No.	Symbols	Parameters	Range
1	$S_p$	Size of silt particles, $\mu$	90 $\mu$ – 600 $\mu$
2	$C_s$	Concentration of silt particles, ppm	2000 ppm – 10000 ppm
3	$V_j$	Velocity of jet, m/s	27.309 m/s - 27.352 m/s
4	$t_w$	Working time, hrs	3-15 hrs

**Governing Equations**

Considering the range of parameters discussed above, experimentations were carried out for various combinations of parameters and data was collected. The data were collected for all the values concentration of silt, size of silt, angle of nozzle and velocity of jet for a time interval of two hours of turbine operation. Sample calculations for one set of readings were given in Appendix A1.

**Calculation of silt concentration:**

Size of the tank:

Length of the Tank: 65 cm

Width of the tank: 52cm

Height of the tank: 80cm water level)

Sand concentration: 10,000ppm

(i) Volume of water in the tank

$$= 68 \times 53 \times 81 \text{ cc} = 270.400 \text{ cc} = 270 \text{ L}$$

(ii) 10,000 ppm = 10,000 mg in one litre

$$10,000 \text{ ppm in } 270 \text{ L} = 10 \times 270 \text{ gm} = 2.7 \text{ kg of silt}$$

**Determination of Jet Velocity:**

The jet velocity was calculated from the reading of pressure transducer observed during the experimentation as follows; Pressure head  $P = \rho gH$

$$\text{Or } H = \frac{P}{\rho g} \tag{1}$$

$$V = k_v \sqrt{2gH} \tag{2}$$

**Measurement of Blade Mass Loss**

(i) Bucket mass loss = Mass of bucket before experiment - Mass of bucket after experiment  
The bucket mass loss was normalized with the bucket mass before the respective experimental run.

(ii) Normalized bucket mass loss

$$= \text{Bucket mass loss} / \text{Mass of bucket before experiment run}$$

**Discharge calculation:**

The formula used for calculating the discharge is as given below (Bansal, 2008)

$$Q = \frac{2}{3} C_e b_e \sqrt{2gh_e} \tag{3}$$

The effective width and head are defined by the following equations;

$$b_e = b + k_b \tag{4}$$

$$h_e = h + k_h \tag{5}$$

**Preference Selection Index (PSI) approach**

This approach designed by Maniya and Bhatt [46] which supports the decision maker to select the suitable alternate. In current study, the ranking of different substitutes has been executed for optimization of operational parameters and a optimum set of geometric factors has been obtained by using PSI approach. The methodology adopted in this study involves two steps and is determined as follow [34], [40] and [41]:

**Step 1: Determination of alternatives and criterions**

In this step alternatives and their variant criterions used for evaluating performance of specific MCDM are identified.

**Step 2: Ranking of different alternatives by using PSI approach**

This PSI approach of alternatives ranking involves different phases in order to calculate the perfect set of experimental results by using number of equations as shown below. The PSI approach involves seven different phases to determine the ranking of alternatives.

**Phase I: Decision matrix**

Decision matrix is designed once different criterions and alternatives are identified. Here A represents alternatives and C signifies criterions. Decision matrix having an order  $A \times C$  is given as:

$$M_{A \times C} = \begin{matrix} A_1 \\ A_2 \\ \dots \\ A_a \end{matrix} \begin{bmatrix} D_{11} & D_{12} & K & D_{1C} \\ D_{21} & D_{22} & K & D_{2C} \\ M & M & K & M \\ D_{A1} & D_{A2} & K & D_{AC} \end{bmatrix} \tag{8}$$

**Phase II: Normalized decision matrix**

In order to make simple comparison of criterions, the decision matrix data has been normalized with a series of [0, 1]. The normalized data of each value in decision matrix is determined as:

$$\begin{cases} X_{ij} = \frac{X_{ij}}{X_j^{max}}, \text{ for larger the better condition} \\ X_{ij} = \frac{X_j^{min}}{X_{ij}}, \text{ for smaller the better condition} \end{cases} \tag{9}$$

**Phase III: Computation of mean results:**

In this part the data of decision matrix is computed by multiplying the mean values of normalized decision matrix with the ration of number of alternatives as:



$$\Delta_j = \frac{1}{A} \sum_{i=1}^a X_{ij} \quad (10)$$

**Phase IV: Calculation of preference deviation ( $\vartheta_j$ ):**

The value of  $\vartheta_j$  for each criterion is determined by subtracting the column wise decision matrix from mean results of normalized decision matrix and after the square root of these values their mean values are obtained as follow:

$$\vartheta_j = \sqrt{\sum_{i=1}^A [X_{ij} - \Delta_j]^2} \quad (11)$$

**Phase V: Calculation of deviation in preference difference ( $\phi_j$ ):**

The value of  $\phi_j$  are determined from following relation:

$$\phi_j = 1 - \frac{\vartheta_j}{A-1} \quad (12)$$

**Phase VI: Determination of whole preference selection values ( $\psi_j$ ):**

The value of  $\psi_j$  are determined from following relation:

$$\theta_j = \frac{\phi_j}{\sum_{j=1}^c \phi_j} \quad (13)$$

Moreover, the entire preference selection value of all criterions is 1 and is given as  $\sum_{j=1}^c \phi_j = 1$

**Phase VII: Calculation of preference selection index values**

The preference selection index ( $\chi_i$ ) values for each alternative are obtained as follow:

$$\chi_i = \sum_{j=1}^c (X_{ij} \times \theta_j) \quad (14)$$

At the end of the calculations of  $\chi_i$ , each alternative is ranked and an alternative with a highest value of  $\chi_i$  is ranked as 1.

**Technique for order preference by similarity to an ideal solution (TOPSIS) approach**

TOPSIS is a popular multi criteria decision making method and multipurpose approach involving a unassuming mathematical model [43], [44] and [45].

**Step 1:** To create evaluation matrix containing m alternatives and n criteria, given by  $x_{ij}$ , as specified below

$$\begin{bmatrix} x_{11} & x_{12} & \dots & x_{1n} \\ x_{21} & x_{22} & \dots & x_{2n} \\ \dots & \dots & \dots & \dots \\ x_{m1} & x_{m2} & \dots & x_{mn} \end{bmatrix} \quad (15)$$

**Step 2:** To normalized above evaluation matrix to form the matrix  $R = (r_{ij})_{m \times n}$  using the normalization method

$$r_{ij} = \frac{x_{ij}}{\sqrt{\sum_{i=1}^m x_{ij}^2}} \quad (16)$$

Where  $i = 1, 2, \dots, m$  and  $j = 1, 2, \dots, n$  The matrix would be given as

$$\begin{bmatrix} r_{11} & r_{12} & \dots & r_{1n} \\ r_{21} & r_{22} & \dots & r_{2n} \\ \dots & \dots & \dots & \dots \\ r_{m1} & r_{m2} & \dots & r_{mn} \end{bmatrix} \quad (17)$$

**Step 3:** To assign a weight factor for each criterion. This weight factor is to be determined objectively by the sum of all weight factors and is equal to 1.

A weighted matrix is to be created to form a matrix where

$$\alpha_{ij} = w_j r_{ij} = w_j \frac{x_{ij}}{\sqrt{\sum_{i=1}^m x_{ij}^2}} \quad (18)$$

Where  $i = 1, 2, \dots, m$  and  $j = 1, 2, \dots, n$  and synthesis weight  $W_j$  for the  $j^{\text{th}}$  attribute is:

$$W_j = \frac{\alpha_j \times \beta_j}{\sum_{j=1}^n \alpha_j \times \beta_j} \quad j = 1, 2, \dots, n \quad (19)$$

The matrix would be given as

$$\begin{bmatrix} \alpha_{11} & \alpha_{12} & \dots & \alpha_{1n} \\ \alpha_{21} & \alpha_{22} & \dots & \alpha_{2n} \\ \dots & \dots & \dots & \dots \\ \alpha_{m1} & \alpha_{m2} & \dots & \alpha_{mn} \end{bmatrix} \quad (20)$$

**Step 4:** Determine the positive ideal solution ( $A_j^+$ ) and the negative ideal solution ( $A_j^-$ ) for each criterion. The coordinates for ( $A_j^+$ ) of positive ideal solution  $A^+ = (A_1^+, A_2^+ \dots \dots A_n^+)$  are chosen using the formula

$$A_j^+ = \begin{cases} \max \alpha_{ij} \text{ for } j = 1, \dots, k \\ \min \alpha_{ij} \text{ for } j = k + 1, \dots, n \end{cases} \quad (21)$$

The coordinates for ( $A_j^-$ ) of positive ideal solution  $A^- = (A_1^-, A_2^- \dots \dots A_n^-)$  are chosen using the formula

$$A_j^- = \begin{cases} \min \alpha_{ij} \text{ for } j = 1, \dots, k \\ \max \alpha_{ij} \text{ for } j = k + 1, \dots, n \end{cases} \quad (22)$$

**Step 5:** Calculate the distance between the target alternative  $i$  and the positive ideal solution  $S^+$  is given by

$$S^+ = \sqrt{\sum_{j=1}^n (a_{ij} - A_j^+)^2} \quad (23)$$

Similarly, calculate the distance between the target alternative  $i$  and the negative ideal solution  $S^-$  is given by

$$S^- = \sqrt{\sum_{j=1}^n (a_{ij} - A_j^-)^2} \quad (24)$$

**Step 6:** Calculate the relative distance of the points from the ideal solution using the formula

$$S = \frac{S^-}{S^+ + S^-} \quad (25)$$

**Step 7:** Rank the S in the descending order with the highest valued criteria/option/alternative being an ideal one.

**IV. RESULTS AND DISCUSSION**

To find erosive wear rate on Pelton turbine, experimentation has been performed among blends of exploratory factors as portrayed in Table 2. After the examination of every elective which is parametric arrangement of erosive wear rate on Pelton turbine, the outcomes have been noted and ascertained for Normalized wear (W) and loss of efficiency. Table.2 describes Normalized wear (W) and efficiency loss reactions accomplished for all alternatives combinations. The surface conditions of turbine bucket after the examination are appeared in Fig.5. The consequences of Table 2 have been introduced in Figures 6 & 7 in order to watch the slant of Normalized wear (W) and efficiency loss contrast simultaneously. It has been discovered that where the efficiency loss is enhanced, in the meantime the estimation of Normalized wear (W) has additionally moved forward.



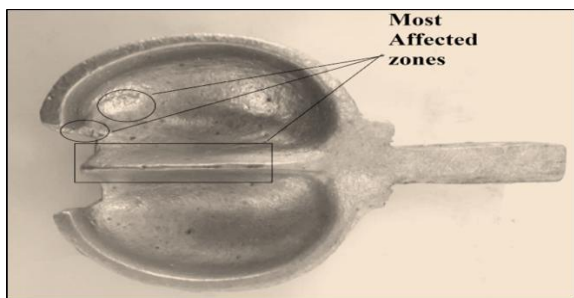


Figure 5. Condition of the bucket after experimentation

Table 2 Experimental results details

Sr. No.	Silt Concentration (ppm)	Silt size ( $\mu$ )	Time period (hrs)	Jet velocity (m/s)	Weight loss (gms)	Efficiency (%age)	Normalized Wear (gms)
1.	2000	90	3	27.309	0.47848	67.206	0.0002443
2.	2000	150	6	27.323	0.61904	64.962	0.0005868
3.	2000	300	9	27.333	0.78442	62.464	0.0010541
4.	2000	450	12	27.344	0.91294	59.845	0.0016697
5.	2000	600	15	27.352	1.11234	59.556	0.0012513
6.	4000	90	6	27.333	1.21216	66.829	0.0010982
7.	4000	150	9	27.344	1.30502	64.492	0.0018151
8.	4000	300	12	27.352	1.43002	61.917	0.0026284
9.	4000	450	15	27.309	1.41798	59.347	0.0027669
10.	4000	600	3	27.323	1.58879	59.065	0.0023480
11.	6000	90	9	27.352	2.10780	66.130	0.0028371
12.	6000	150	12	27.309	2.26072	63.657	0.0040621
13.	6000	300	15	27.323	2.24214	61.142	0.0041528
14.	6000	450	3	27.333	2.08978	58.720	0.0031113
15.	6000	600	6	27.344	2.27034	58.404	0.0026830
16.	8000	90	12	27.323	2.75412	65.096	0.0040469
17.	8000	150	15	27.333	2.76602	62.646	0.0048589
18.	8000	300	3	27.344	2.20660	60.766	0.0011646
19.	8000	450	6	27.352	2.38800	57.932	0.0020784
20.	8000	600	9	27.309	2.71968	57.503	0.0051067
21.	10000	90	12	27.344	3.41301	64.686	0.0061570
22.	10000	150	3	27.352	3.43504	61.756	0.0070269
23.	10000	300	6	27.309	3.13406	59.879	0.0038560
24.	10000	450	9	27.323	3.34410	56.843	0.0047169
25.	10000	600	15	27.333	3.74979	56.813	0.0079370

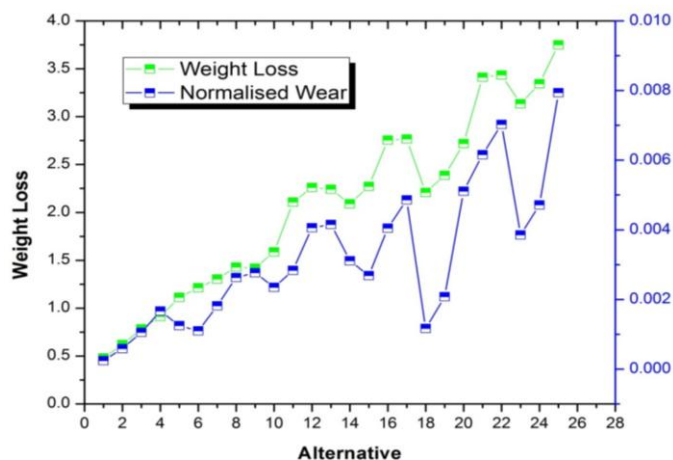


Figure 6. Difference of experimental results with alternatives

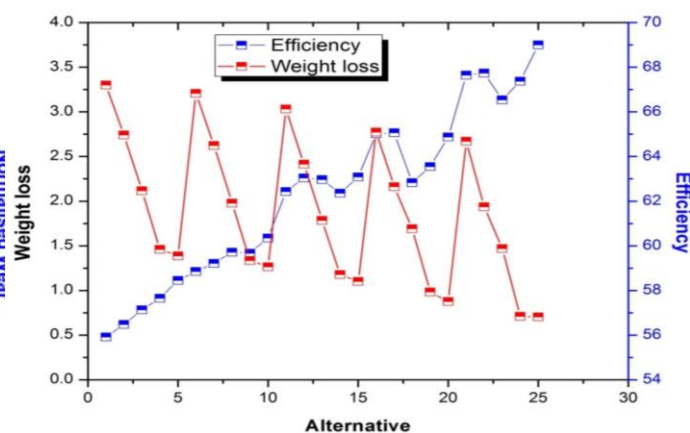


Figure 7. Difference of experimental results with alternatives

**Numerical calculation for optimization of results**

**PSI technique**

The criterion obtained from experimental investigation of erosive wear rate parameters in Pelton turbine bucket has been analyzed respectively. The different stages of simulation process are depicted below:

**Elementary decision matrix:**

The number of experimental runs is calculated as alternatives A-1 to A-25 and the criterion such as Weight loss, Efficiency, Normalized Wear are measured as C-1, C-2 and C-3 respectively for performance measurement of erosive wear rate parameters in Pelton turbine bucket. A resulting elementary decision matrix ( $M_{A \times C}$ ) has been designed where A represents the number of alternatives and C represents the number of criterions. The resulting column wise decision matrix is depicted as below:

$$M_{A \times C} = \begin{matrix} A_1 \\ A_2 \\ A_3 \\ A_4 \\ A_5 \\ M \\ A_{25} \end{matrix} \begin{bmatrix} 0.47848(C_{11}) & 67.206(C_{12}) & 0.0002443(C_{13}) \\ 0.61904(C_{21}) & 64.962(C_{22}) & 0.0005868(C_{23}) \\ 0.78442(C_{31}) & 62.464(C_{32}) & 0.0010541(C_{33}) \\ 0.91294(C_{41}) & 59.845(C_{42}) & 0.0016697(C_{43}) \\ 1.11234(C_{51}) & 59.556(C_{52}) & 0.0012513(C_{53}) \\ M & M & M \\ 3.74979(C_{A1}) & 56.813(C_{A2}) & 0.0079370(C_{AC}) \end{bmatrix} \quad (26)$$

After the calculation and design of decision matrix, the maximum criterion represented as  $(X_j)_{max}$  and minimum criterion represented as  $(X_j)_{min}$  has been determined by using Eq. (9):

$$(X_j)_{max} = \max_i X_{ij} = [3.74979 \quad 67.206 \quad 0.007937]$$

$$(X_j)_{min} = \min_i X_{ij} = [0.47848 \quad 56.813 \quad 0.0002443]$$

**Calculation of column-wise normalized decision matrix:**

After the identification of highest and lowest values of criterions the normalized values of whole data in decision matrix are determined by employing Eq. (10) and the results of normalized values are shown in Table 3.

**Table 3 Normalized Decision Matrix**

Alternative	C-1	C-2	C-3
A-1	1	1	1
A-2	0.772939	0.96661	0.416326
A-3	0.609979	0.929441	0.231762
A-4	0.524109	0.890471	0.146314
A-5	0.430156	0.886171	0.195237
A-6	0.394733	0.99439	0.222455
A-7	0.366646	0.959617	0.134593
A-8	0.334597	0.921302	0.092946
A-9	0.337438	0.883061	0.088294
A-10	0.30116	0.878865	0.104046
A-11	0.227004	0.98399	0.086109
A-12	0.211649	0.947192	0.060141
A-13	0.213403	0.90977	0.058828
A-14	0.228962	0.873732	0.07852
A-15	0.210753	0.86903	0.091055
A-16	0.173732	0.968604	0.060367
A-17	0.172985	0.932149	0.050279

A-18	0.21684	0.904175	0.209772
A-19	0.200369	0.862006	0.117542
A-20	0.175932	0.855623	0.047839
A-21	0.140193	0.962503	0.039678
A-22	0.139294	0.918906	0.034766
A-23	0.152671	0.890977	0.063356
A-24	0.143082	0.845802	0.051792
A-25	0.127602	0.845356	0.03078

**Calculation of column-wise data:**

The standardized values of normalized decision matrix have been determined by Eq. (10)

$$\Delta_{C-1} = 0.04 \times 7.806229 = 0.312249$$

$$\Delta_{C-2} = 0.04 \times 22.87974 = 0.91519$$

$$\Delta_{C-3} = 0.04 \times 3.712798 = 0.148512$$

**Calculation of preference deviation data:**

The preference deviation data ( $\vartheta_j$ ) for each criterion is determined with the help of Eq. (11)

$$\vartheta_{C-1} = 1.114559$$

$$\vartheta_{C-2} = 0.053934$$

$$\vartheta_{C-3} = 0.93569$$

**Calculation of deviation in preference difference values:**

The deviation in preference difference values ( $\phi_j$ ) is calculated for every response by using Eq. (12):

$$\phi_{C-1} = 1 - \frac{1.114559}{24} = 0.95356$$

$$\phi_{C-2} = 1 - \frac{0.053934}{24} = 0.997753$$

$$\phi_{C-3} = 1 - \frac{0.93569}{24} = 0.961013$$

**Calculation of whole preference selection values ( $\theta_j$ ):**

The values of  $\theta_j$  are determined with the help of equation (13):

$$\theta_{C-1} = \frac{0.95356}{2.912326} = 0.327422$$

$$\theta_{C-2} = \frac{0.997753}{2.912326} = 0.342597$$

$$\theta_{C-3} = \frac{0.961013}{2.912326} = 0.329981$$

**Table 4 Optimization results of Preference deviation data, Preference difference values and Whole preference selection values**

Criteria	Preference deviation data ( $\vartheta_C$ )	Preference difference values ( $\phi_C$ )	Whole preference selection values ( $\theta_C$ )
Criteria - 1	1.114559	0.95356	0.327422
Criteria - 2	0.053934	0.997753	0.342597
Criteria - 3	0.93569	0.961013	0.329981

**Calculation of preference selection index ( $\chi_i$ ) data**

The PSI ( $\chi_i$ ) results for whole alternatives are determined by employing equation (14). The alternative having highest value of  $\chi_i$  is selected as optimum set of geometric parameters.



# Selection of Erosive Wear Rate Parameters of Pelton Turbine Buckets using PSI and TOPSIS Techniques

It is found that  $\chi_i$  of alternative A-1 is maximum (0.9999) followed by A-2 (0.721567) among all alternative. The alternative A-25 depicts the minimum value of PSI having preference index value equal to 0.721567. The above examinations show that the alternative A-1 has an optimal set of geometric parameters i.e. silt concentration = 2,000 silt size = 90, time period = 3 hrs. and jet velocity = 27.309 which shows the best performance. The responses achieved in the form of rank after computations are shown in Table 5.

**Table 5 PSI ( $\chi_i$ ) and rank of the alternatives**

Alternative	Preference index ( $\chi_i$ )	Rank
A-1	0.9999	1
A-2	0.721567	2
A-3	0.594592	3
A-4	0.524938	5
A-5	0.508844	6
A-6	0.543302	4
A-7	0.493207	7
A-8	0.455848	8
A-9	0.442142	10
A-10	0.434024	12
A-11	0.439843	11
A-12	0.413643	13
A-13	0.400963	14
A-14	0.400206	16
A-15	0.396769	18
A-16	0.408639	15
A-17	0.392577	19
A-18	0.449968	9
A-19	0.399701	17
A-20	0.366519	23
A-21	0.388743	20
A-22	0.371891	22
A-23	0.376134	21
A-24	0.353703	24
A-25	0.34155	25

## TOPSIS Technique

### Determination of weight for different criteria

The subjective weight ( $\alpha_j$ ) calculated using pairwise comparisons are given in Table 6. After the determination of  $\alpha_j$ , the objective weight ( $\beta_j$ ) is determined by using entropy method. From the values of  $\alpha_j$  and  $\beta_j$  the value of synthesis weight ( $\omega_j$ ) for each attributes is calculated by using Eq. (19) are given in Table 7.

**Table 6: The pair wise comparison matrix for different criteria's**

	C-1	C-2	C-3
C-1	0.22	0.22	0.25
C-2	0.67	0.65	0.63
C-3	0.11	0.13	0.13

**Table 7: The criteria weights subjective ( $\alpha_j$ ), objective ( $\beta_j$ ), and synthesis weight ( $\omega_j$ )**

	C-1	C-2	C-3
$\alpha_j$	0.230	0.648	0.122
$\beta_j$	0.329	0.392	0.279

$w_j$	0.208	0.698	0.094
-------	-------	-------	-------

## Calculation of Normalized and Weighted Normalized Decision Matrix

In application of TOPSIS method the decision matrix of criteria given in Eq. (26) is normalized using Eq. (16). The each column of this normalized matrix is multiplied by corresponding synthesis weight ( $w_j$ ) to find weighted normalized matrix given in Table 8.

**Table 8: Normalized and weighted normalized matrix**

Alternative	Normalized Decision Matrix			Weighted Normalized Decision Matrix		
	C-1	C-2	C-3	C-1	C-2	C-3
A-1	0.0088	0.1523	0.0012	0.0088	0.1523	0.0012
A-2	0.0113	0.1473	0.0029	0.0113	0.1473	0.0029
A-3	0.0144	0.1416	0.0052	0.0144	0.1416	0.0052
A-4	0.0167	0.1357	0.0083	0.0167	0.1357	0.0083
A-5	0.0204	0.1350	0.0062	0.0204	0.1350	0.0062
A-6	0.0222	0.1515	0.0054	0.0222	0.1515	0.0054
A-7	0.0239	0.1462	0.0090	0.0239	0.1462	0.0090
A-8	0.0262	0.1404	0.0130	0.0262	0.1404	0.0130
A-9	0.0260	0.1345	0.0137	0.0260	0.1345	0.0137
A-10	0.0291	0.1339	0.0116	0.0291	0.1339	0.0116
A-11	0.0386	0.1499	0.0140	0.0386	0.1499	0.0140
A-12	0.0414	0.1443	0.0201	0.0414	0.1443	0.0201
A-13	0.0411	0.1386	0.0205	0.0411	0.1386	0.0205
A-14	0.0383	0.1331	0.0154	0.0383	0.1331	0.0154
A-15	0.0416	0.1324	0.0133	0.0416	0.1324	0.0133
A-16	0.0505	0.1476	0.0200	0.0505	0.1476	0.0200
A-17	0.0507	0.1420	0.0240	0.0507	0.1420	0.0240
A-18	0.0404	0.1377	0.0058	0.0404	0.1377	0.0058
A-19	0.0438	0.1313	0.0103	0.0438	0.1313	0.0103
A-20	0.0498	0.1303	0.0253	0.0498	0.1303	0.0253
A-21	0.0625	0.1466	0.0305	0.0625	0.1466	0.0305
A-22	0.0629	0.1400	0.0348	0.0629	0.1400	0.0348
A-23	0.0574	0.1357	0.0191	0.0574	0.1357	0.0191
A-24	0.0613	0.1288	0.0233	0.0613	0.1288	0.0233
A-25	0.0687	0.1288	0.0393	0.0687	0.1288	0.0393

**Determination of the positive ideal solution ( $A_j^+$ ) and the negative ideal solution ( $A_j^-$ )**

The value of positive ideal solutions ( $A_j^+$ ) and negative ideal solutions ( $A_j^-$ ) of each criteria determined from weighted normalized matrix using Eqs. (21) and (22) are given in Table 9.

**Table 9: Positive ideal solutions ( $A_j^+$ ) and negative ideal solutions ( $A_j^-$ ) each criteria.**

	PDA-1	PDA-2	PDA-3
$A_j^+$	0.0088	0.1523	0.0012
$A_j^-$	0.0687	0.1288	0.0393

**Determination of relative distance and ranking of the alternatives**

After finding  $A_j^+$  and  $A_j^-$  the target distances of each alternative  $S_i^+$  and  $S_i^-$  calculated for all alternatives using Eqs. (23) and (24) are given in Table 10. Finally, the relative distance of the points from the ideal solution ( $S$ ) of all alternatives is calculated using Eq. (25) and results are given in Table 10. In the end after whole calculation the ranking of alternatives done to get optimal set of operating parameters presented in in Table 10.

**Table 10: Target distances, relative distance and ranking of the alternatives**

Alternative	$S_+$	$S_-$	$S$	Rank
A-1	0.000	0.075	0.999	1
A-2	0.006	0.070	0.923	2
A-3	0.013	0.065	0.837	3
A-4	0.020	0.061	0.755	6
A-5	0.021	0.059	0.733	7
A-6	0.014	0.062	0.814	4
A-7	0.018	0.057	0.759	5
A-8	0.024	0.051	0.680	8
A-9	0.028	0.050	0.644	9
A-10	0.029	0.049	0.624	10
A-11	0.033	0.045	0.578	11
A-12	0.039	0.037	0.488	14
A-13	0.040	0.035	0.465	17
A-14	0.038	0.039	0.506	13
A-15	0.040	0.038	0.484	15
A-16	0.046	0.032	0.414	18
A-17	0.049	0.027	0.357	19
A-18	0.035	0.045	0.560	12
A-19	0.042	0.038	0.479	16
A-20	0.052	0.024	0.310	20
A-21	0.061	0.021	0.253	22
A-22	0.065	0.013	0.171	24
A-23	0.054	0.024	0.308	21
A-24	0.062	0.018	0.222	23
A-25	0.075	0.000	0.001	25

It has been found that alternative A-1 has maximum relative distance (0.999) from all the alternatives and is followed by A-2 (0.923) alternative. The alternative A-25 depicts the minimum value of relative distance equal to 0.721567. The above inspections show that the alternative A-1 has an optimal set of geometric parameters i.e. silt concentration = 2,000 silt size = 90, time period = 3 hrs and jet velocity = 27.309 which shows the best performance. Figure 8 shows the

rankings of all alternatives derived using PSI and TOPSIS methods.

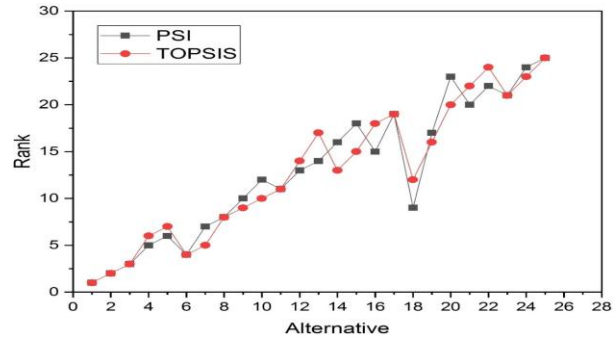


**Figure 8. Comparisons of ranking obtained with the PSI and TOPSIS methods**

**Conclusion**

In this study, PSI and TOPSIS approaches has been carried out to investigate the effects of wear rate on silt size and silt concentration in a Pelton turbine buckets. The PSI technique calculates the preference variance values and deviation in preference variance values of all the performance approximation criterions towards whole performance. The PSI technique ranked the whole alternatives by giving a significant solution which is nearest to real value and faraway from the least values. The experimental results exhibit variant capabilities for each alternative investigated, thus the PSI technique was employed to give an optimal set of alternatives on which structure will provided maximum performance with minimum energy inputs. Based up on the results obtained from both PSI and TOPSIS approaches it is found that optimal performance has been provided by A-1 alternative with geometric and flow parameters as  $S_p = 90 \mu$ ,  $C_s = 2000 ppm$ ,  $V_j = 27.309 m/s$  and  $t_w = 3 hrs$  respectively.

**REFERENCES**

- V. K. Singh and S. K. Singal, "Operation of hydro power plants-a review," *Renew. Sustain. Energy Rev.*, vol. 69, November 2016, pp. 610–619, 2017.
- D. Robb, "Hydro's fish-friendly turbines," *Renew. Energy Focus*, vol. 12, no. 2, pp. 16–17, 2011.
- M. Bansal, D. K. Khatod, and R. P. Saini, "Modeling and optimization of integrated renewable energy system for a rural site," in *2014 International Conference on Reliability Optimization and Information Technology (ICROIT)*, 2014, pp. 25–28.
- A. Pundir and A. Kumar, "Technical feasibility study for power generation from a potential mini hydro site nearby Shoolini University," vol. 2, no. 2, pp. 85–95, 2014.
- D. J. Woodcock and I. Morgan White, "The application of pelton type impulse turbines for energy recovery on sea water reverse osmosis systems," *Desalination*, vol. 39, no. C, pp. 447–458, 1981.
- R. Chattopadhyay, "High silt wear of hydroturbine runners," *Wear*, vol. 162–164, no. PART B, pp. 1040–1044, 1993.
- B. S. Mann, "High-energy particle impact wear resistance of hard coatings and their application in hydroturbines," *Wear*, vol. 237, no. 1, pp. 140–146, 2000.
- B. S. Mann and V. Arya, "Abrasive and erosive wear characteristics of plasma nitriding and HVOF coatings: Their application in hydro turbines," *Wear*, vol. 249, no. 5–6, pp. 354–360, 2001.
- G. R. Desale, B. K. Gandhi, and S. C. Jain, "Effect of erodent properties on erosion wear of ductile type materials," *Wear*, vol. 261, no. 7–8, pp. 914–921, 2006.
- T. R. Bajracharya, B. Acharya, C. B. Joshi, R. P. Saini, and O. G. Dahlhaug, "Sand erosion of Pelton turbine nozzles and buckets: A case study of Chilime Hydropower Plant," *Wear*, vol. 264, no. 3–4, pp. 177–184, 2008.



# Selection of Erosive Wear Rate Parameters of Pelton Turbine Buckets using PSI and TOPSIS Techniques

11. A. K. Chauhan, D. B. Goel, and S. Prakash, "Erosion behaviour of hydro turbine steels," *Bull. Mater. Sci.*, vol. 31, no. 2, pp. 115–120, 2008.
12. D. Agar and M. Rasi, "On the use of a laboratory-scale Pelton wheel water turbine in renewable energy education," *Renew. Energy*, vol. 33, no. 7, pp. 1517–1522, 2008.
13. [M. K. Padhy and R. P. Saini, "Effect of size and concentration of silt particles on erosion of Pelton turbine buckets," *Energy*, vol. 34, no. 10, pp. 1477–1483, 2009.
14. B. S. Thapa, B. Thapa, and O. G. Dahlhaug, "Current research in hydraulic turbines for handling sediments," *Energy*, vol. 47, no. 1, pp. 62–69, 2012.
15. J. S. Anagnostopoulos and D. E. Papantonis, "A fast Lagrangian simulation method for flow analysis and runner design in Pelton turbines," *J. Hydrodyn.*, vol. 24, no. 6, pp. 930–941, 2012.
16. D. K. Goyal, H. Singh, H. Kumar, and V. Sahni, "Slurry erosive wear evaluation of HVOF-spray Cr2O3coating on some turbine steels," *J. Therm. Spray Technol.*, vol. 21, no. 5, pp. 838–851, 2012.
17. M. K. Padhy and R. P. Saini, "Study of silt erosion mechanism in Pelton turbine buckets," *Energy*, vol. 39, no. 1, pp. 286–293, 2012.
18. S. J. Williamson, B. H. Stark, and J. D. Booker, "Performance of a low-head pico-hydro Turgo turbine," *Appl. Energy*, vol. 102, pp. 1114–1126, 2013.
19. B. R. Cobb and K. V. Sharp, "Impulse (Turgo and Pelton) turbine performance characteristics and their impact on pico-hydro installations," *Renew. Energy*, vol. 50, pp. 959–964, 2013.
20. S. Khurana and V. Goel, "Effect of jet diameter on erosion of turgo impulse turbine runner," *J. Mech. Sci. Technol.*, vol. 28, no. 11, pp. 4539–4546, 2014.
21. C. A. Platero, C. Nicolet, J. A. Sánchez, and B. Kawkabani, "Increasing wind power penetration in autonomous power systems through no-flow operation of Pelton turbines," *Renew. Energy*, vol. 68, pp. 515–523, 2014.
22. A. Židonis and G. A. Aggidis, "State of the art in numerical modelling of Pelton turbines," *Renew. Sustain. Energy Rev.*, vol. 45, pp. 135–144, 2015.
23. D. Kumar and P. P. Bhingole, "CFD Based Analysis of Combined Effect of Cavitation and Silt Erosion on Kaplan Turbine," *Mater. Today Proc.*, vol. 2, no. 4–5, pp. 2314–2322, 2015.
24. R. kumar and S. K. Singal, "Operation and Maintenance Problems in Hydro Turbine Material in Small Hydro Power Plant," *Mater. Today Proc.*, vol. 2, no. 4–5, pp. 2323–2331, 2015.
25. J. C. Chávez, J. A. Valencia, G. A. Jaramillo, J. J. Coronado, and S. A. Rodríguez, "Failure analysis of a Pelton impeller," *Eng. Fail. Anal.*, vol. 48, pp. 297–307, 2015.
26. A. Židonis, A. Panagiotopoulos, G. A. Aggidis, J. S. Anagnostopoulos, and D. E. Papantonis, "Parametric optimisation of two Pelton turbine runner designs using CFD," *J. Hydrodyn.*, vol. 27, no. 3, pp. 403–412, 2015.
27. A. Židonis and G. A. Aggidis, "Pelton turbine: Identifying the optimum number of buckets using CFD," *J. Hydrodyn.*, vol. 28, no. 1, pp. 75–83, 2016.
28. V. B. Nguyen, Q. B. Nguyen, Y. W. Zhang, C. Y. H. Lim, and B. C. Khoo, "Effect of particle size on erosion characteristics," *Wear*, vol. 348–349, pp. 126–137, 2016.
29. V. Gupta, V. Prasad, and R. Khare, "Numerical simulation of six jet Pelton turbine model," *Energy*, vol. 104, pp. 24–32, 2016.
30. C. Vessaz, L. Andolfatto, F. Avellan, and C. Tournier, "Toward design optimization of a Pelton turbine runner," *Struct. Multidiscip. Optim.*, vol. 55, no. 1, pp. 37–51, 2017.
31. M. Egusquiza, E. Egusquiza, D. Valentin, C. Valero, and A. Presas, "Failure investigation of a Pelton turbine runner," *Eng. Fail. Anal.*, vol. 81, no. September 2016, pp. 234–244, 2017.
32. A. M. Morales B, I. F. Pachón, J. Loboguerrero U, J. A. Medina, and J. A. Escobar G, "Development of a test rig to evaluate abrasive wear on Pelton turbine nozzles. A case study of Chivor Hydropower," *Wear*, vol. 372–373, pp. 208–215, 2017.
33. B. Kishor, G. P. Chaudhari, and S. K. Nath, "Slurry erosion behaviour of thermomechanically treated 16Cr5Ni stainless steel," *Tribol. Int.*, vol. 119, no. November 2017, pp. 411–418, 2018.
34. K. Maniya and M. G. Bhatt, "A selection of material using a novel type decision-making method: Preference selection index method," *Mater. Des.*, vol. 31, no. 4, pp. 1785–1789, 2010.
35. R. Chauhan, T. Singh, N. S. Thakur, and A. Patnaik, "Optimization of parameters in solar thermal collector provided with impinging air jets based upon preference selection index method," *Renew. Energy*, vol. 99, pp. 118–126, 2016.
36. B. Vahdani, S. M. Mousavi, and S. Ebrahimnejad, "Soft computing-based preference selection index method for human resource management," *J. Intell. Fuzzy Syst.*, vol. 26, no. 1, pp. 393–403, 2014.
37. R. Attri, N. Dev, K. Kumar, and A. Rana, "Selection of cutting-fluids using a novel decision-making method: preference selection index method," *Int. J. Inf. Decis. Sci.*, vol. 6, no. 4, p. 393, 2014.
38. Mesran, K. Tampubolon, R. D. Sianturi, F. T. Waruwu, and A. P. U. Siahaan, *Determination of Education Scholarship Recipients Using Preference Selection Index*, vol. 3, no. 6, 2017.
39. M. Madić, J. Antucheviciene, M. Radovanović, and D. Petković, "Determination of laser cutting process conditions using the preference selection index method," *Opt. Laser Technol.*, vol. 89, pp. 214–220, 2017.
40. J. R. Lockwood, "On the statistical analysis of multiple-choice feeding preference experiments," *Oecologia*, vol. 116, no. 4, pp. 475–481, 1998.
41. K. D. Maniya and M. G. Bhatt, "The selection of flexible manufacturing system using preference selection index method," *Int. J. Ind. Syst. Eng.*, vol. 9, no. 3, p. 330, 2011.
42. E. Roszkowska, "Multi-Criteria Decision Making Models by applying the TOPSIS Method to crisp and interval data," *Mult. Criteria Decis. Mak.*, vol. 6, no. Mcdm, pp. 200–230, 2011.
43. O. Management, "A review on industrial applications of TOPSIS approach Santosh Kumar Yadav \*, Dennis Joseph and Nasina Jigeesh," vol. 30, no. 1, 2018.
44. S. Opricovic and G. H. Tzeng, "Compromise solution by MCDM methods: A comparative analysis of VIKOR and TOPSIS," *Eur. J. Oper. Res.*, 2004.
45. M. Behzadian, S. Khanmohammadi Otaghsara, M. Yazdani, and J. Ignatius, "A state-of-the-art survey of TOPSIS applications," *Expert Syst. Appl.*, 2012.
46. K. D. Maniya and M. G. Bhatt, "An alternative multiple attribute decision making methodology for solving optimal facility layout design selection problems," *Comput. Ind. Eng.*, vol. 61, no. 3, pp. 542–549, 2011.

## AUTHORS PROFILE



**Robin Thakur**, He is currently working as an associate professor in Shoolini University, Solan. His qualifications includes B.Tech (Mechanical Engineering), M.Tech (Manufacturing Technology & Automation) & PhD (Mechanical Engineering). He has specialization in Hydro Turbines, Thermal Engineering & Mechanics. He has published several papers in reputed international journals and attended so many conferences. He has 13 years of Teaching & Industrial Experience. He also filed 7 patents in his field and 2 of them are granted by government of India.



**Sunil Kumar** is working as Assistant Professor, Shoolini University, Solan, India. He received M. Tech. degree in engineering education from Panjab University Chandigarh and pursuing PhD from Uttarakhand Technical University, Dehradun, India. He has published more than 15 research papers in international and national level. Currently working on heat transfer, fluid flow characteristics and properties of different Nanofluids in heat exchangers. Research work is based on numerical and experimental studies in developing new heat transfer fluids as well as heat transfer enhancement techniques for saving energy.



**Ashwani Kumar**, He is currently working as an Assistant Professor in ECE Deptt. in Shoolini University, Solan (H.P). He has submitted PhD in University of Petroleum & Energy Studies, Dehradun (U.K) in Computer Sciences. He has also served Green Hills Engineering College as an assistant professor for 4 years and as a Quality and testing Engineer in Cenzar Industries Pvt. Ltd. He has published several papers in reputed international journals and attended so many conferences. His area of research is optical fiber communication, Basic Electronics & Digital Signal Processing. He has also filed several patents on his work.



**Kamal Kashyap** is a Ph.D. scholar at Shoolini University. He has published various papers in national and international journals. His area of interest is Hydro turbines, Eco friendly energy and Energy generation from traditional technologies.



**Sorabh Aggarwal** is working as Assistant Professor, Shoolini University, Solan, India. He Received M. Tech degree in Mechanical Engineering from NIT Kurukshetra. He has total of 6 Years of teaching experience, He has filed 25 patents in the field of Mechanical Engineering and 5 of them have been granted.